Journal of Alloys and Compounds 509 (2011) 4754–4764

Contents lists available at ScienceDirect

Journal of Alloys and Compounds

journal homepage: www.elsevier.com/locate/jallcom

Preparation and photocatalytic activity of immobilized composite photocatalyst (titania nanoparticle/activated carbon)

Niyaz Mohammad Mahmoodi[a,b,*], Mokhtar Arami[a,*], Jason Zhang[c]

[a] Textile Engineering Department, Amirkabir University of Technology, Tehran, Iran
[b] Department of Environmental Research, Institute for Color Science and Technology, Tehran, Iran
[c] Department of Chemical & Biological Engineering, University of Ottawa, Ottawa, Canada

ARTICLE INFO

Article history:
Received 3 October 2010
Received in revised form 17 January 2011
Accepted 21 January 2011
Available online 2 February 2011

Keywords:
Immobilized composite photocatalyst
Titania nanoparticle/activated carbon (AC)
Preparation
Photocatalytic activity
Degradation
Mineralization

ABSTRACT

An immobilized composite photocatalyst, titania (TiO_2) nanoparticle/activated carbon (AC), was prepared and its photocatalytic activity on the degradation of textile dyes was tested. AC was prepared using *Canola* hull. Basic Red 18 (BR18) and Basic Red 46 (BR46) were used as model dyes. Fourier transform infrared (FTIR), wavelength dispersive X-ray spectroscopy (WDX), scanning electron microscopy (SEM), UV–vis spectrophotometry, chemical oxygen demand (COD) and ion chromatography (IC) analyses were employed. The effects of reaction parameters such as weight percent (wt.%) of activated carbon, pH, dye concentration and anions (NO_3^-, Cl^-, SO_4^{2-}, HCO_3^- and CO_3^{2-}) were investigated on dye degradation. Data showed that dyes were decolorized and degraded using novel immobilized composite photocatalyst. Formate, acetate and oxalate anions were detected as dominant aliphatic intermediates where, they were further oxidized slowly to CO_2. Nitrate, chloride and sulfate anions were detected as the photocatalytic mineralization products of dyes. Results show that novel immobilized composite photocatalyst with 2 wt.% of AC is the most effective novel immobilized composite photocatalyst to degrade of textile dyes.

1. Introduction

Azo dyes, which contain one or more azo bonds (–N=N–), are among the most widely used synthetic dyes and usually become major pollutants in textile wastewaters. About 15% of the total world production of dyes is lost during textile dyeing which is released in textile effluents. The discharge of dye-bearing wastewater from textile industries into natural stream and rivers poses severe problems, because of toxicity of some dyes to the aquatic life and damaging to the aesthetic nature of the environment [1–10]. Thus, there is an urgent need for textile wastewater to develop effective methods of treatment.

Titania photocatalysis constitutes one of the emerging technologies for the degradation of organic pollutants [10–17]. TiO_2 nanoparticles can be synthesized by precipitation from solutions of either titanium salts or titanium alkoxides [13].

Several advantages of this process over competing processes are: (1) complete mineralization, (2) no waste-solids disposal problem, and (3) only mild temperature and pressure conditions are necessary [10–17].

Titania photodegrades pollutant molecules when is radiated with UV radiation. Researchers have discovered that during the photodegradation process, interaction by certain pollutant molecules or their intermediates could cause the titania to coagulate, thereby reducing the amount of UV radiation from reaching the titania active centers (due to reduction of its surface area) and thus reducing its catalytic effectiveness. In order to overcome this coagulation problem, some researchers have used different materials as a support for the titania photocatalyst [17,18]. Various substrates have been used as a catalyst support for the photocatalytic degradation of polluted water. For example glass materials: glass mesh, glass fabric, glass wool [19], glass beads [20], glass reactors [21], microporous cellulosic membranes [22], ceramic membranes [23], monoliths [14], zeolites [25] and stainless steel [26] were used as a support for titania.

Activated carbon (AC) is a porous, amorphous solid carbon material, which is derived mainly from carbonaceous material or plant based (lignocellulosic) material [17]. Activated carbons have also been extensively researched to be used as a support [17–34] for the TiO_2 photocatalyst. Besides being used as a catalyst support, some researchers use a combination of TiO_2 and activated carbon suspensions to treat pollutant [17,35–43]. Activated carbon increases the photodegradation rate by progressively allowing an increased quantity of substrate to come in contact with the titania through means of adsorption. This is important because it has been established that the oxidizing species (•OH) generated by the pho-

* Corresponding authors at: Textile Engineering Department, Amirkabir University of Technology, Tehran, Iran. Tel.: +98 021 22969771; fax: +98 021 22947537.
E-mail addresses: nm_mahmoodi@aut.ac.ir, nm_mahmoodi@yahoo.com (N.M. Mahmoodi).

0925-8388/$ – see front matter © 2011 Elsevier B.V. All rights reserved.
doi:10.1016/j.jallcom.2011.01.146

tocatalyst, does not migrate very far from the active centers of the titania and therefore degradation takes place on the catalyst surface. The adsorption of pollutant to be then transfer by a common interface from AC to TiO_2 it was firstly pointed out by Matos et al. [40].

Activated carbon will prove to be an invaluable support in promoting the photocatalytic process in providing a synergistic effect by creating a common interface between both the activated carbon phase and the titania particle phase. The synergistic effect can be explained as an enhanced adsorption of the target pollutant onto the activated carbon phase followed closely by a transfer through an interphase to the titania phase, giving a complete photodegradation process [17].

Organic compounds are hydrophobic whereas titania particles, when exposed to UV radiation, are hydrophilic. Using activated carbons as a photocatalyst support will help bring the pollutant molecules near to the titania active site (to come in contact with the hydroxyl radicals) for an efficient and effective photodegradation process (synergistic effect). Activated carbons can generate new adsorption centers to favor approaching pollutant molecules. In addition, using activated carbon as a support will enable secondary degradation of intermediates to take place in situ, further enhancing the effectiveness of the photocatalyst [17].

However, in the large scale applications, the use of suspensions requires the separation and recycling of the catalyst particles from the treated wastewater prior to the discharge and can be a time-consuming expensive process. In addition, the depth of penetration of UV light is limited because of strong absorptions by both catalyst particles and dissolved dyes [44]. Above problems can be avoided by immobilization of photocatalyst over a suitable support.

A literature review showed that the preparation and photocatalytic activity of immobilized composite photocatalyst (titania nanoparticle/*Canola* hull activated carbon) was not investigated. In this study, Activated carbon (AC) was prepared from *Canola* hull and a novel immobilized composite photocatalyst, titania nanoparticle–*Canola* hull activated carbon (AC), was prepared and its photocatalytic activity on the degradation of textile dye in aqueous solution was tested. Basic Red 18 (BR18) and Basic Red 46 (BR46) were used as model dyes. Fourier transform infrared (FTIR), wavelength dispersive X-ray spectroscopy (WDX), scanning electron microscopy (SEM), UV–vis spectrophotometry, chemical oxygen demand (COD) and ion chromatography (IC) analyses were employed. The effects of reaction parameters such as activated carbon weight percent (wt.%), pH, dye concentration and inorganic anions were investigated on dye degradation.

2. Experimental

2.1. Reagents

Basic Red 18 (BR18) and Basic Red 46 (BR46) were obtained from CIBA. The chemical structure of dyes was shown in Fig. 1. Titania nanoparticle was utilized as a photocatalyst and its main physical data are as follows: average particle size 30 nm, purity above 97% and with 80:20 anatase to rutile. Other chemicals were purchased from Merck and used as received.

2.2. Preparation of Canola hull activated carbon

Canola hull was obtained from a local field in north of Iran. The *Canola* hull was firstly washed to remove the adhering dirt, and then was dried (in a drier for 2 h at 105 °C until a constant weight was reached) and crushed. After drying, they were sieved to the required particle size of <0.125 mm. Then *Canola* hull was soaked in a nitric acid solution (10 wt.%) for 24 h. The sample is then decanted, dried in an oven at 105 °C then carbonized in a muffle furnace for 1 h at 600 °C in the absence of air [7]. The activated carbon treated with HNO_3 was obtained.

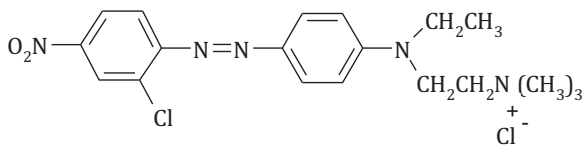

BR18

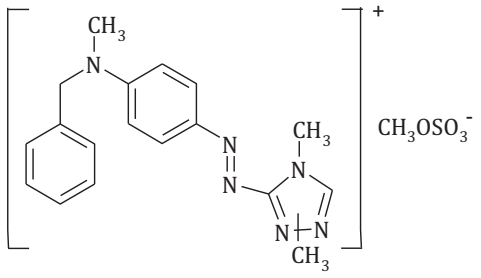

BR46

Fig. 1. The chemical structure of dyes.

2.3. Preparation of novel composite photocatalyst (TiO_2 nanoparticle–Canola hull activated carbon) and immobilization method

Titania nanoparticle was mixed with different *Canola* hull activated carbon weight percent. A simple and effective method was used to immobilization of novel composite photocatalyst as follows: inner surfaces of reactor walls were cleaned with acetone and distilled water to remove any organic or inorganic material attached to or adsorbed on the surface and dried in the air. A pre-measured mass of titania nanoparticle–*Canola* hull activated carbon was attached on the inner surfaces of reactor walls using a thin layer of a UV resistant polymer. Immediately after preparation, the inner surface reactor wall – polymer – composite photocatalyst system was placed in the laboratory for at least 60 h for complete drying of the polymer.

2.4. Characterization techniques

In order to investigate the surface characteristics of the prepared *Canola* hull activated carbon and novel composite photocatalyst, Fourier transform infra-red (FTIR), wavelength dispersive X-ray spectroscopy (WDX) and scanning electron microscopy (SEM) were used. Fourier transform infrared (FTIR) spectroscopy is a useful in identifying functional groups such as hydroxyl, carbonyl and aromatic rings in a variety of samples. FTIR (Perkin-Elmer Spectrophotometer Spectrum One) in the range 450–4000 cm^{-1} was studied. Wavelength dispersive X-ray spectroscopy (WDX) was employed to obtain information on the content of atoms for example titanium and carbon in the samples. WDX spectroscopy (CROSPEC – USA) was employed to obtain information on the content of titanium and carbon in the composite photocatalyst samples. Scanning electron microscopy (SEM) has been a primary tool for characterizing the surface morphology and fundamental physical properties of the adsorbent surface. SEM observations were obtained using a Philips XL30 microscope instrument.

2.5. Photocatalytic reactor

Experiments were carried out in a batch mode immersion rectangular immobilized novel composite photocatalyst photocatalytic reactor made of Pyrex glass. The radiation source was two UV-C lamps (200–280 nm, 15 W Philips). The schematic representation of the reactor was in previous published paper [4].

2.6. Photocatalytic dye degradation

Photocatalytic degradation processes were performed using a 5 L solution containing specified concentration of dye. The initial concentration of dye was 0.128 mM and 0.120 mM for BR18 and BR46, respectively. Samples were withdrawn from sample point at certain time intervals and analyzed for decolorization and degradation.

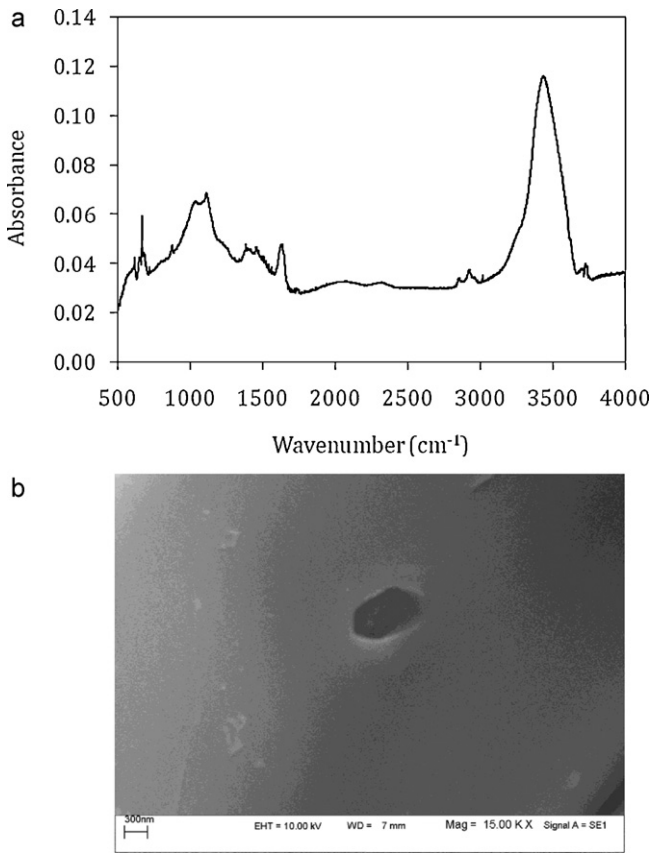

Fig. 2. *Canola* hull activated carbon (a) FTIR spectrum (b) SEM.

Decolorization of dye solution was checked and controlled by measuring the absorbance at maximum wavelength (λ_{max}) of dyes (488 nm for BR18 and 532 nm for BR46) at different time intervals by UV–vis spectrophotometer (CECIL 2021).

The COD tests were carried out according to close reflux, colorimetric method [45] using a DR/2500 spectrophotometer (Hach, USA) and COD reactor (Hach, USA).

Ion chromatograph (METROHM 761 Compact IC) was used to assay the appearance and quantity of formate, acetate, oxalate, sulfate and nitrate ions formed during the degradation and mineralization of AR 14 using an METROSEP anion dual 2, flow 0.8 mL/min, 2 mM $NaHCO_3$/1.3 mM Na_2CO_3 as eluent, temperature 20 °C, pressure 3.4 MPa and conductivity detector.

3. Results and discussions

3.1. Characterization of Canola hull activated carbon (AC) and novel immobilized composite photocatalyst (titania nanoparticle–Canola hull activated carbon)

In order to investigate the surface characteristics of *Canola* hull activated carbon, Fourier transform infrared in the range 450–4000 cm^{-1} and SEM image were studied (Fig. 2). The FTIR spectrum of AC shows that the peak positions are at 3442.16, 2916.76, 2845.41, 1632.43, 1113.51 and 1022.70 cm^{-1}. The band at 3442.16 cm^{-1} is due to O–H and N–H stretching. The bands at 2916.76 and 2845.41 cm^{-1} correspond to unsymmetrical and symmetrical aliphatic C–H stretchings, respectively. While the band at 1632.43 cm^{-1} reflects C=C stretching of aromatic rings whose intensity is enhanced by the presence of oxygen atoms as phenol or ether groups. Bands at 1300–1000 cm^{-1} correspond to C–O bending and indicate the presence of phenolic groups [46–50]. SEM image of *Canola* hull activated carbon shows that AC has homogenous surface (Fig. 2b).

Table 1
Parameters (k and R^2) for the effect of H_2O_2 concentration on the photocatalytic decolorization of dyes using immobilized composite photocatalyst (2 wt.% of AC) (BR18: dye: 0.128 mM, λ_{max}: 488 nm and BR46: dye: 0.120 mM, λ_{max}: 532 nm).

H_2O_2 (mM)	BR18		BR46	
	k (min^{-1})	R^2	k (min^{-1})	R^2
5	0.0413	0.9758	0.1000	0.9950
7.68 (stoichiometry)	0.0850	0.9878	0.1722	0.9764
10	0.0979	0.9898	0.1968	0.9932

SEM images of the immobilized novel composite photocatalyst show that composite photocatalyst was immobilized on inner surface of reactor (Fig. 3).

WDX images of novel composite photocatalyst showed the content of titanium and carbon at different samples (Fig. 4). Fig. 4a and e are the WDX images of immobilized pure titania nanoparticle and pure *Canola* hull activated carbon, respectively. Fig. 4b–d are the images of novel composite photocatalysts with 1, 2 and 3 wt.% *Canola* hull activated carbon. It can be seen that the number of light spots (*C*: carbon atom at right images in Fig. 4) increases with increasing of wt.% of AC. It can be concluded that the AC was mixed with titania nanoparticles in novel composite photocatalyst.

3.2. Effects of reaction parameters on dye degradation

The effects of reaction parameters such as H_2O_2, *Canola* hull activated carbon wt.%, pH, dye concentration, and anions (NO_3^-, Cl^-, SO_4^{2-}, HCO_3^- and CO_3^{2-}) were investigated on dye degradation.

3.2.1. Effect of hydrogen peroxide concentration

Hydrogen peroxide has different effects on the photocatalytic dye decomposition, depending on its concentration and nature of reluctant.

Fig. 5 shows the dye concentration as a function of the illumination time when different hydrogen peroxide concentrations were used. It is shown to be exponential to time at each hydrogen peroxide concentration. This means that the first order kinetics relative to dye degradation is operative. The correlation coefficient (R^2) and degradation rate constants (k, min^{-1}) of dye for the various hydrogen peroxide concentrations were shown in Table 1.

At optimal concentration, H_2O_2 increases the formation rate of hydroxyl radicals and pollutant degradation. However, at high concentration, H_2O_2 can also become a scavenger of valence bond holes and hydroxyl radicals [51–53].

$$H_2O_2 + 2h_{VB}^+ \rightarrow O_2 + 2H^+ \quad (1)$$

$$H_2O_2 + OH^\bullet \rightarrow HO_2^\bullet + H_2O \quad (2)$$

$$HO_2^\bullet + OH^\bullet \rightarrow H_2O + O_2 \quad (3)$$

The overall stoichiometry for photocatalytic mineralization of dyes by H_2O_2 can be written as:

$$C_{19}H_{25}Cl_2N_5O_2 + 60H_2O_2 \rightarrow 19CO_2 + 5NO_3^- + 69H_2O + 7H^+ + 2Cl^- \quad (BR18) \quad (4)$$

$$C_{19}H_{24}N_6O_4S + 64H_2O_2 \rightarrow 19CO_2 + 6NO_3^- + SO_4^{2-} + 72H_2O + 8H^+ \quad (BR46) \quad (5)$$

On the basis of these equations, 60 and 64 mol of H_2O_2 are theoretically needed to completely degrade 1 mol of BR18 and BR46, respectively. Thus for further studies, 60 and 64 mol of H_2O_2 were used to degrade 1 mol of BR18 and BR46, respectively.

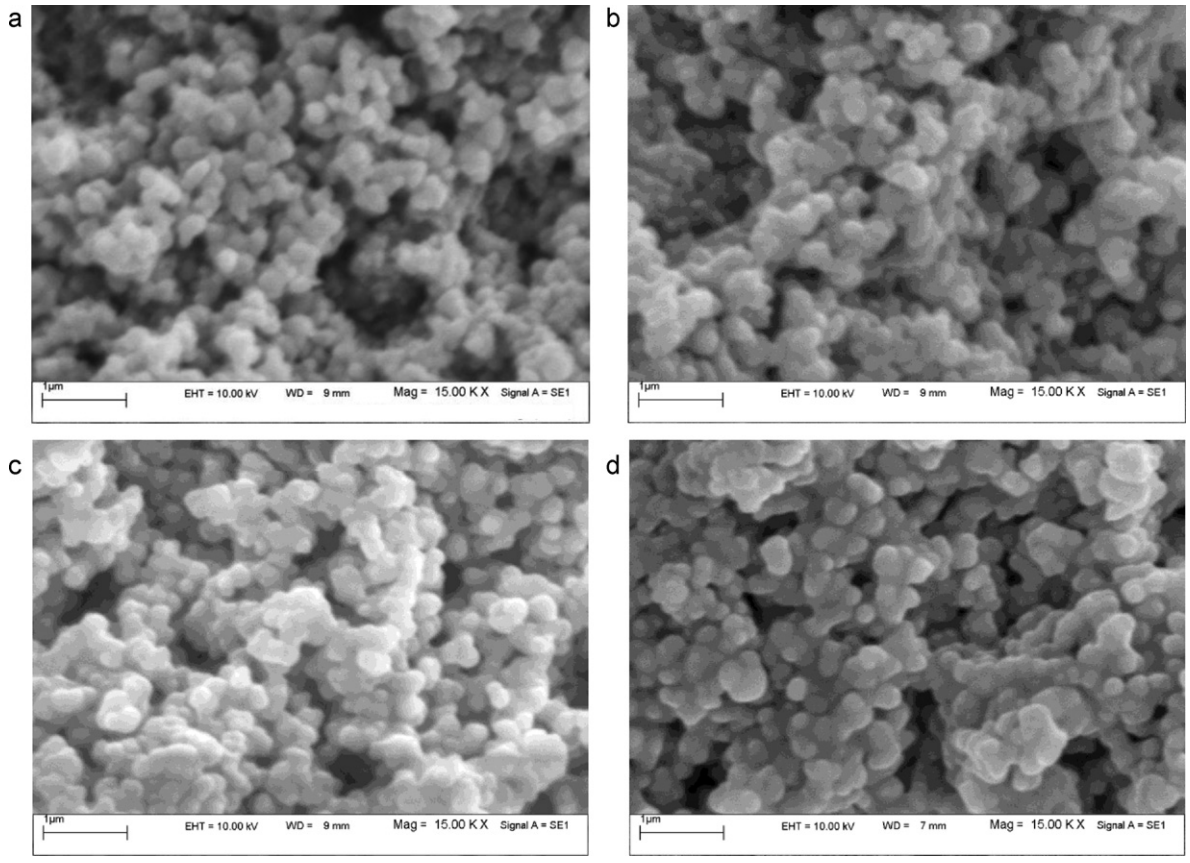

Fig. 3. SEM of immobilized composite photocatalyst (titania nanoparticle–*Canola* hull activated carbon) at different wt.% of *Canola* hull activated carbon: (a) 0 (b) 1 (c) 2 (d) 3.

3.2.2. Effect of Canola hull activated carbon wt.%

Fig. 6 shows the dye concentration as a function of the illumination time when different *Canola* hull activated carbon wt.% on novel composite photocatalyst were used. It is shown to be exponential to time at each *Canola* hull activated carbon wt.%. This means that the first order kinetics relative to dye degradation is operative. The correlation coefficient (R^2) and degradation rate constants (k, min^{-1}) of dye for the various *Canola* hull activated carbon wt.% were shown in Table 2. The disappearance of the color within first minutes is due to the fragmentation of the azo band, which is the result of hydroxyl radical (•OH) attack. This process is the first step in the degradation of azo dye.

The chemical oxygen demand (COD) gives a measure of degradation of dye and generated intermediates during the irradiation and a measure of the oxygen equivalent of the organic content in a sample that is susceptible to oxidation by strong oxidant [54]. The COD removal efficiency of dyes using immobilized pure titania nanoparticle and immobilized novel composite photocatalyst (titania nanoparticle–*Canola* hull activated carbon) were shown in Table 3.

Table 2
Parameters (k and R^2) for the effect of *Canola* hull activated carbon wt.% on the photocatalytic decolorization of dyes using immobilized composite photocatalyst (H_2O_2: 7.68 mM, BR18: dye: 0.128 mM, λ_{max}: 488 nm, pH: 5.5 and BR46: dye: 0.120 mM, λ_{max}: 532 nm, pH: 5.6).

AC (wt.%)	BR18		BR46	
	k (min^{-1})	R^2	k (min^{-1})	R^2
0	0.0588	0.9839	0.1408	0.9775
1	0.0728	0.9935	0.1642	0.9453
2	0.0850	0.9878	0.1722	0.9764
3	0.0996	0.9544	0.1836	0.9756
6	0.1049	0.9522	0.1925	0.9750
12	0.1075	0.9530	0.2029	09718

(a) Results show that as *Canola* hull activated carbon wt.% of composite photocatalyst increases, the decolorization rate and COD removal enhance. From the results here presented it can be concluded that the chemical nature of the AC is important for the degradation process, which can be explained in terms of two different mechanisms [55]:
(b) The dye adsorption on the AC is followed by a transfer of the compound to the titania where undergoes a photocatalyzed surface reaction of degradation. The driving force for this transfer is probably the difference in the dye concentration between AC and titania causing surface diffusion of the dye to titania.

The AC acts as a photosensitizer which injects an electron in the conduction band of titania and triggers the photocatalytic formation of the very reactive HO• radical, which is responsible for the degradation of the dye.

Data show that immobilized novel composite photocatalyst with 2 and 3 wt.% AC do not have considerable difference in dye and COD removals. Thus, immobilized novel composite photocatalyst with 2 wt.% was used for further studies.

3.2.3. Effect of solution pH

Since dyes to degrade can be at different pH values in colored effluents, comparative experiments were performed at three pH values: one reasonably acidic, one reasonably basic and natural pH.

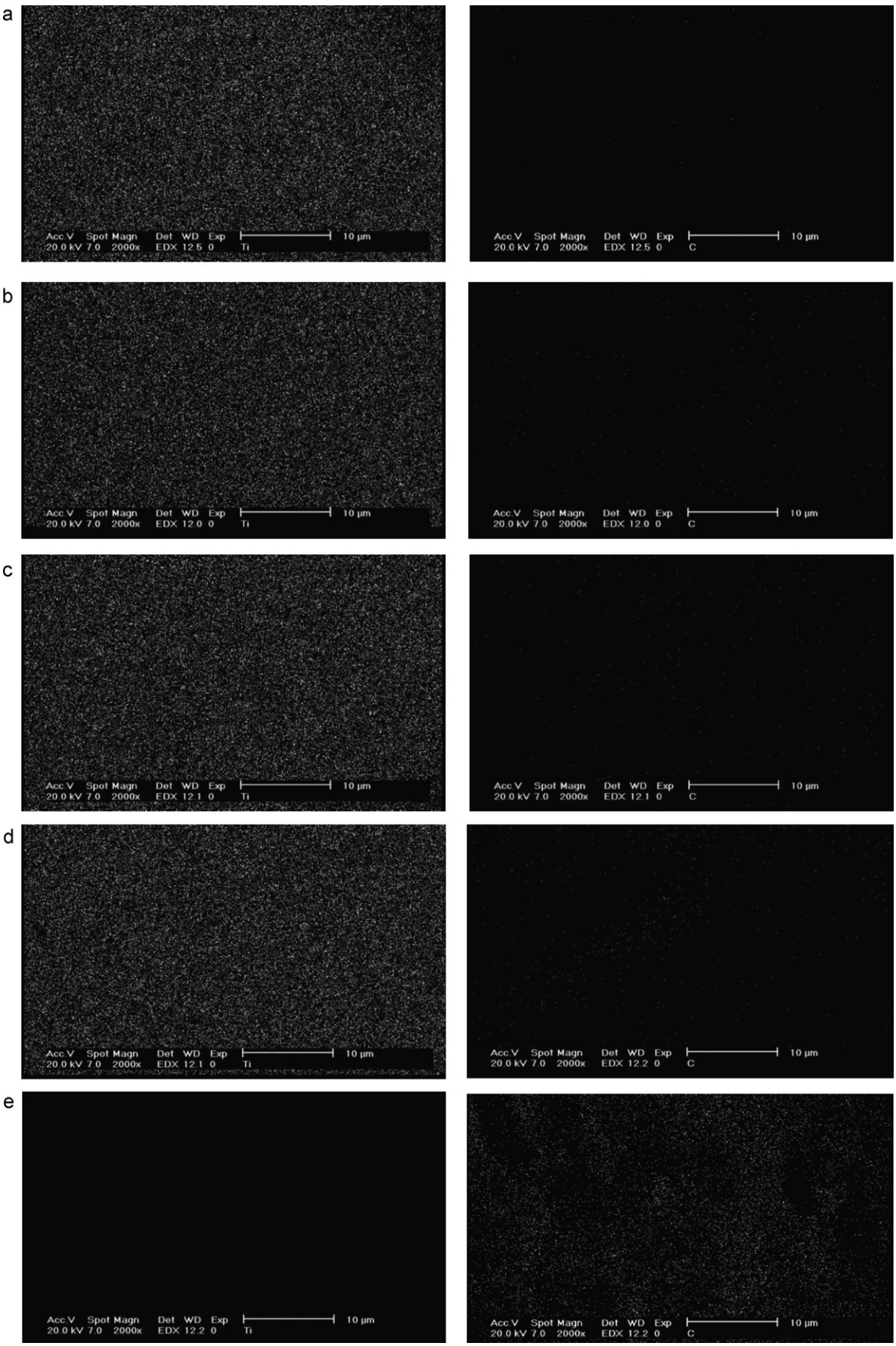

Fig. 4. WDX of immobilized composite photocatalyst (titania nanoparticle–*Canola* hull activated carbon) at different wt.% of *Canola* hull activated carbon: (a) 0, (b) 1, (c) 2, (d) and 3 (e) pure *Canola* hull activated carbon.

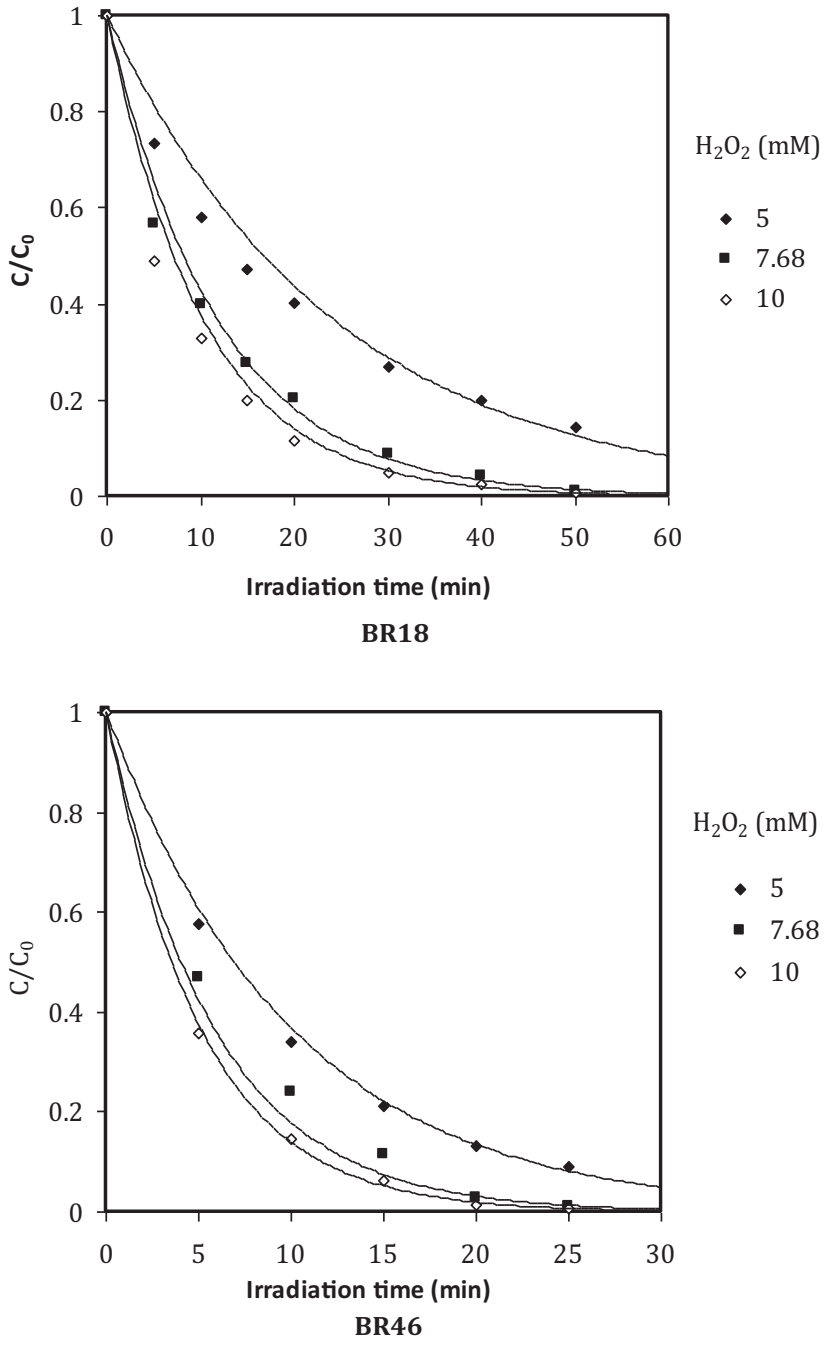

Fig. 5. The effect of H_2O_2 concentration on the photocatalytic decolorization of dyes using immobilized composite photocatalyst (2 wt.% of AC) (BR18: dye: 0.128 mM, λ_{max}: 488 nm and BR46: dye: 0.120 mM, λ_{max}: 532 nm).

Table 3
COD removal (%) by the photocatalytic degradation of dyes using immobilized composite photocatalyst at different *Canola* hull activated carbon wt.% and different times (H_2O_2: 7.68 mM, BR18: dye: 0.128 mM, pH: 5.5 and BR46: dye: 0.120 mM, pH: 5.6).

AC (wt.%)	BR18							BR46						
	COD at different *t* (min)				COD removal (%)			COD at different *t* (min)				COD removal (%)		
	0	50	100	150	50	100	150	0	50	100	150	50	100	150
0	255	215	160	91	15.7	37.2	64.3	248	205	155	105	17.3	37.5	57.7
1		195	120	65	23.5	52.9	74.5		190	110	83	23.4	55.6	66.5
2		185	105	48	27.4	58.8	81.2		181	87	59	27.0	64.9	76.2
3		181	98	40	29.0	61.6	84.3		176	80	50	29.0	67.7	79.8

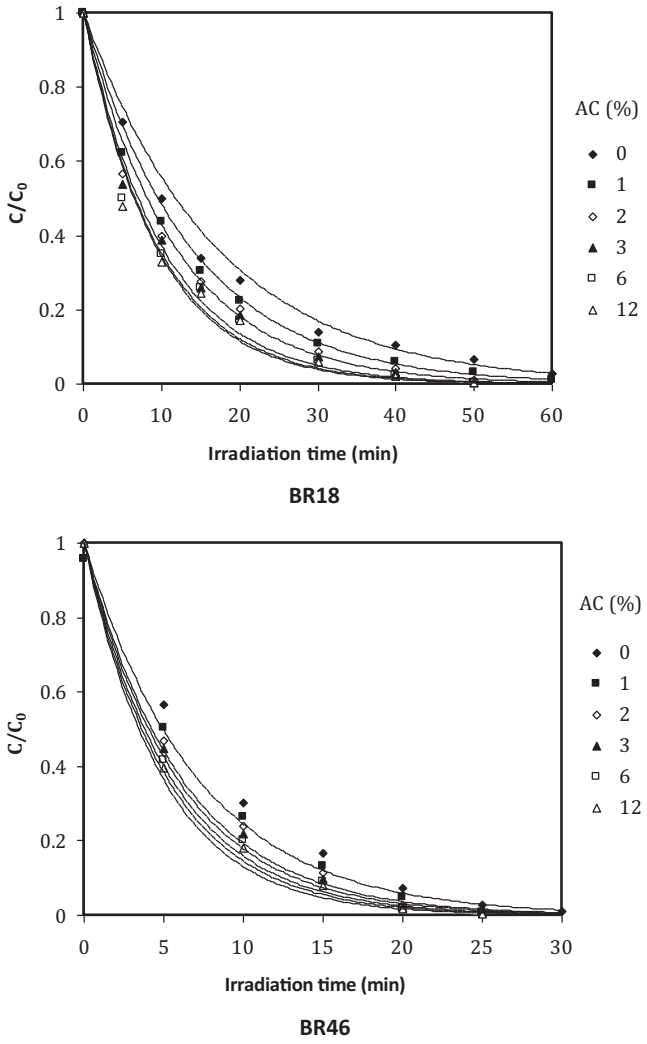

Fig. 6. The effect of *Canola* hull activated carbon (AC) wt.% on the photocatalytic decolorization of dyes using immobilized composite photocatalyst (H_2O_2: 7.68 mM, BR18: dye: 0.128 mM, λ_{max}: 488 nm, pH: 5.5, and BR46: dye: 0.120 mM, λ_{max}: 532 nm, pH: 5.6).

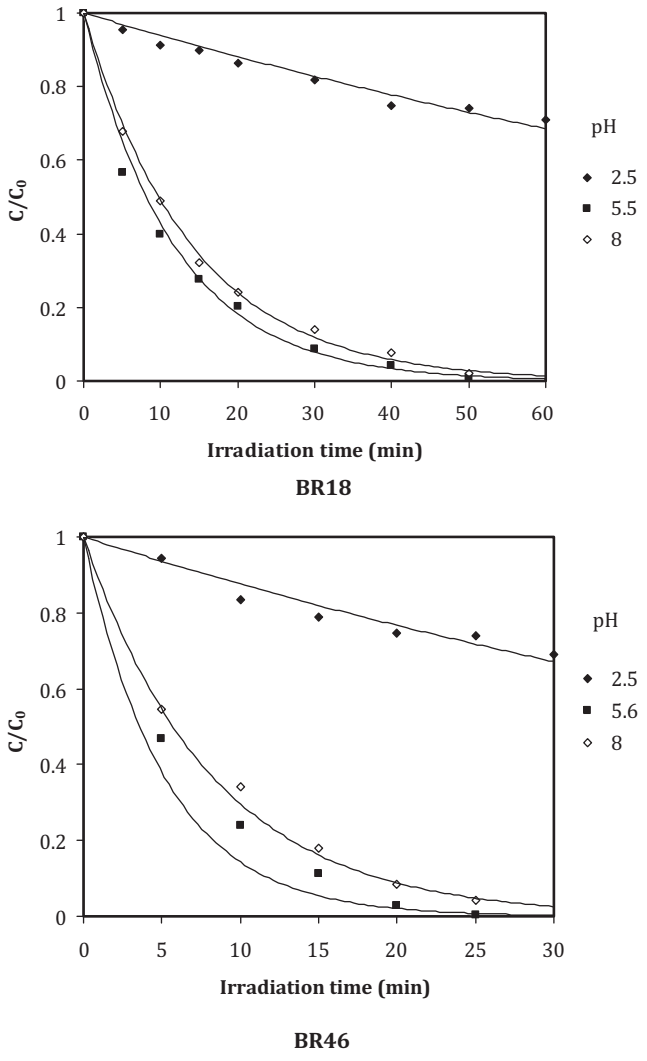

Fig. 7. The effect of pH on the photocatalytic decolorization of dyes using immobilized composite photocatalyst (2 wt.% of AC) (H_2O_2: 7.68 mM, BR18: dye: 0.128 mM, λ_{max}: 488 nm and BR46: dye: 0.120 mM, λ_{max}: 532 nm).

The studies in this report were carried out at pH range of 2–8. The pH of solution is an important parameter in reaction taking place on semiconductor particle surfaces, since it influences the surface charge properties of the photocatalyst. The point of zero charge (pzc) is at $pH_{pzc} = 6.8$ for the TiO_2 particles [56]. The TiO_2 surface is positively charged in acidic media (pH < 6.8). Therefore, an electrostatic repulsion exists between the positively charged surface of the TiO_2 and cationic dyes. As the pH of the system increases, the number of negatively charged sites increased. A negatively charged surface site on the TiO_2 favors the adsorption of dye cations due to the electrostatic attraction. In this research, a novel immobilized composite photocatalyst contained titania nanoparticle and *Canola* hull activated carbon (AC) was used. Surface charge of activated carbon (AC) was changed by solution pH. However the interpretation of pH effects on the efficiency of the photocatalytic decolorization process is a difficult task, because the different reaction mechanisms such as hydroxyl radical attack, direct oxidation by positive hole and direct reduction by the electron in the conducting band can contribute to dye degradation. The importance of each one depends on the substrate nature and pH [57,58].

The effect of pH on the decolorization of dyes is shown in Fig. 7. The parameters k (rate constant) and R^2 (correlation coefficient) of decolorization process are shown in Table 4. As shown in Table 4, the order of rate constants was $pH_{natural} > pH_{alkaline} > pH_{acidic}$. In this study, natural pHs were found to be the optimal pH.

3.2.4. Effect of initial dye concentration

To study the effect of dye concentration on the rate of decolorization, the dye concentration was varied 0.060–0.256 mM while the other variables were kept constant. Fig. 8 shows the time dependence of unconverted fraction of dye (C/C_0: C_0 initial dye concentration and C dye concentration at time t) for the various initial dye concentrations. It is shown to be exponential to time at each concentration of dye. This means that the first order kinetics relative to dye is operative. The correlation coefficient

Table 4
Parameters (k and R^2) for the effect of pH on the photocatalytic decolorization of dyes using immobilized composite photocatalyst (2 wt.% of AC) (H_2O_2: 7.68 mM, BR18: dye: 0.128 mM, λ_{max}: 488 nm and BR46: dye: 0.120 mM, λ_{max}: 532 nm).

pH	BR18		BR46	
	k (min^{-1})	R^2	k (min^{-1})	R^2
2.5	0.0063	0.9603	0.0133	0.9441
5.5 (natural pH)	0.0850	0.9878	–	–
5.6 (natural pH)	–	–	0.1722	0.9764
8	0.0712	0.9814	0.1214	0.9944

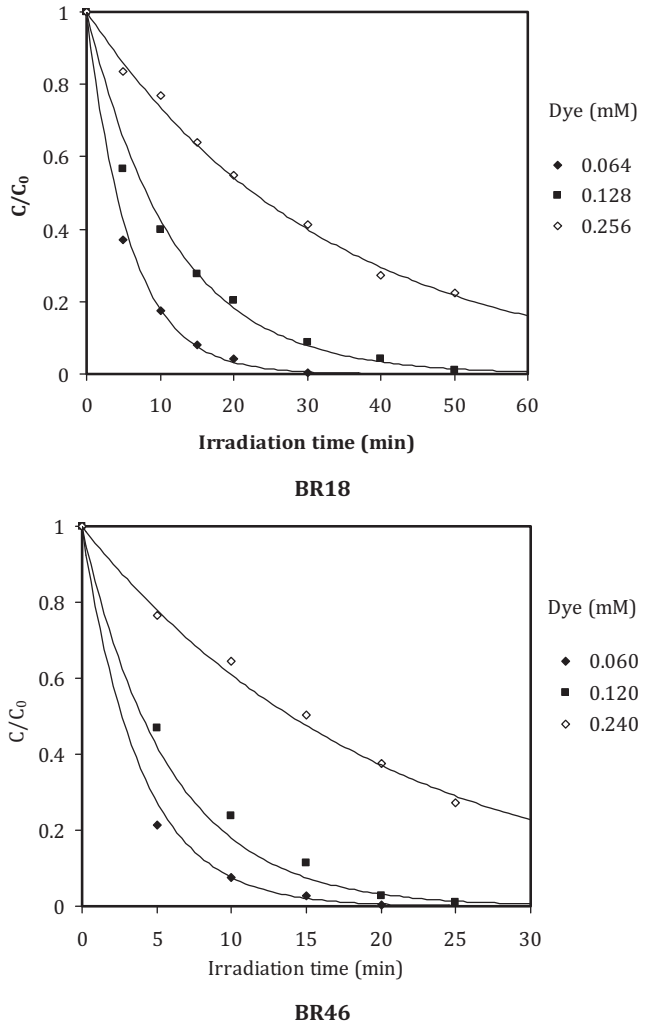

Fig. 8. The effect of dye concentration on the photocatalytic decolorization of dyes using immobilized composite photocatalyst (2 wt.% of AC) (H_2O_2: 7.68 mM, BR18: λ_{max}: 488 nm, pH: 5.5 and BR46: λ_{max}: 532 nm, pH: 5.6).

(R^2) and degradation rate constants (k, min^{-1}) at different dye concentrations were shown in Table 6. However, the apparent decolorization rate constant depends on the initial concentration of dye. As expected by increasing the dye concentration, the decolorization rate constant (k) is decreased (Table 5).

With the increase in the dye concentration, the possible cause is the interference from intermediates formed upon degradation of the parental dye molecules. Such suppression would be more pronounced in the presence of an elevated level of degradation intermediates formed upon an increased initial dye concentration [59].

Table 5
Parameters (k and R^2) for the effect of dye concentration on the photocatalytic decolorization of dyes using immobilized composite photocatalyst (2 wt.% of AC) (H_2O_2: 7.68 mM, BR18: λ_{max}: 488 nm, pH: 5.5 and BR46: λ_{max}: 532 nm, pH: 5.6).

Dye (mM)	BR18		BR46	
	k (min^{-1})	R^2	k (min^{-1})	R^2
0.060	–	–	0.0496	0.9904
0.064	0.1713	0.9935	–	–
0.120	–	–	0.1722	0.9764
0.128	0.0850	0.9878	–	–
0.240	–	–	0.2574	0.9895
0.256	0.0305	0.9948	–	–

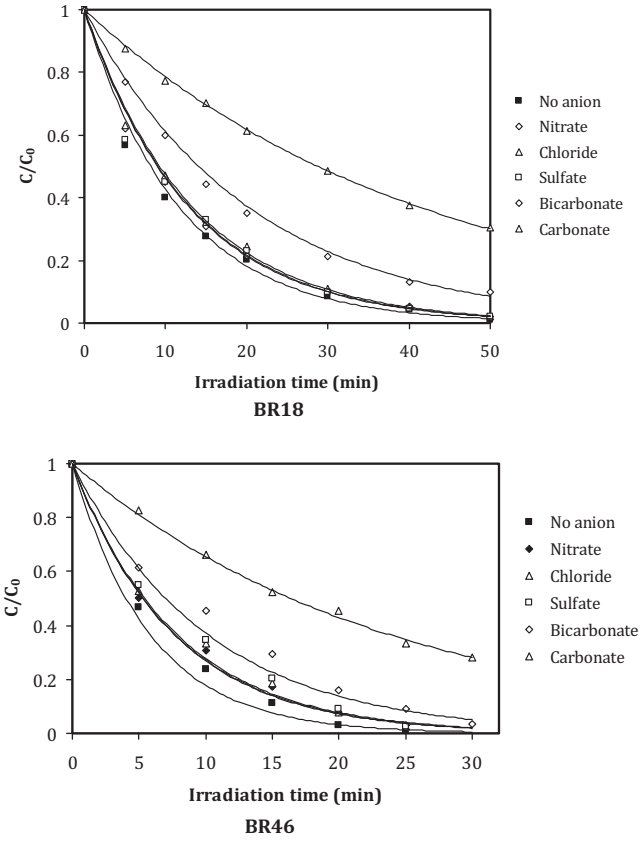

Fig. 9. The effect of anions on the photocatalytic decolorization of dyes using immobilized composite photocatalyst (2 wt.% of AC) (H_2O_2: 7.68 mM, BR18: dye: 0.128 mM, λ_{max}: 488 nm, pH: 5.5 and BR46: dye: 0.120 mM, λ_{max}: 532 nm, pH: 5.6).

3.2.5. Effect of inorganic anions

The occurrence of dissolved inorganic ions is rather common in dye-containing industrial wastewater. These substances may compete for the active sites on the TiO_2 surface or deactivate the photocatalyst and, subsequently, decrease the decolorization rate of the target dyes [10]. A major drawback resulting from the high reactivity and non-selectivity of •OH is that it also reacts with non-target compounds present in the background water matrix, i.e. dye auxiliaries present in the exhausted reactive dye bath. It results higher •OH demand to accomplish the desired degree of degradation, or complete inhibition of advanced oxidation rate and efficiency [60].

To consider how the presence of dissolved inorganic anions on the photocatalytic decolorization rate of dyes, we have chosen the $NaNO_3$, NaCl, Na_2SO_4, $NaHCO_3$ and Na_2CO_3 salts. The same amount (2.5 mM) of these salts was used. Fig. 9 shows the effects of anions on the photocatalytic decolorization rate of dyes. The parameters k (rate constant) and R^2 (correlation coefficient) of decolorization process are shown in Table 6. Of the anionic species studied (NaCl, $NaNO_3$, Na_2SO_4, $NaHCO_3$ and Na_2CO_3), Na_2CO_3 exhibited the strongest inhibition effect followed by $NaHCO_3$. Inhibition effects of anions can be explained as the reaction of positive holes and hydroxyl radical with anions, that behaved as h^+ and •OH scavengers resulting prolonged color removal [10,60].

3.3. UV–vis spectrum studies

Changes of the dyes absorptions at 250 nm ≤ λ ≤ 650 nm during the photocatalytic degradation using immobilized composite photocatalyst (titania nanoparticle–*Canola* hull activated carbon) at different time intervals of irradiation were shown in Fig. 10. With

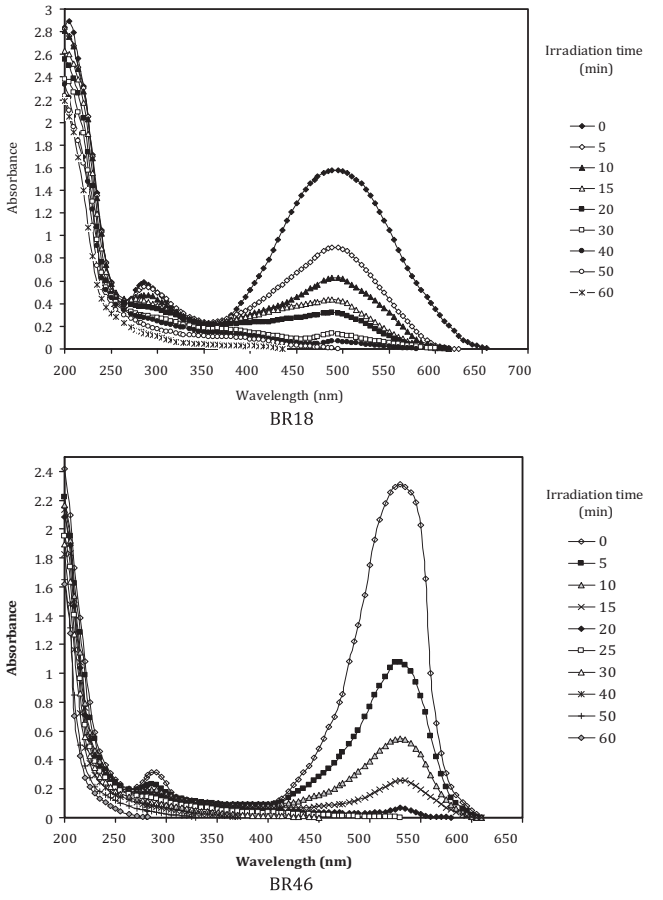

Fig. 10. Changes of the dyes absorptions during the photocatalytic degradation of dyes using immobilized composite photocatalyst (2 wt.% of AC) (H_2O_2: 7.68 mM, BR18: dye: 0.128 mM, λ_{max}: 488 nm, pH: 5.5 and BR46: dye: 0.120 mM, λ_{max}: 532 nm, pH: 5.6).

irradiation time elapse of 50 min, the maximum absorbance in visible region of UV–vis spectra decreased rapidly, which indicates that chromophore in both dyes are the most active sites for oxidation attack. Also, absorbance measurements of the samples at 254 nm were taken as an indication of the aromatic compounds content in the solution [61]. The lack of any absorbance in 254 nm after 80 min and 100 min of photocatalytic degradation of BR46 and BR18 using composite photocatalyst (titania/AC) was indicative of the complete aromatic rings destruction (Fig. 11).

3.4. Degradation and mineralization of dyes

During the photocatalytic degradation of dyes, various organic intermediates were produced. Consequently, destruction of the dye

Table 6
Parameters (k and R^2) for the effect of anions on the photocatalytic decolorization of dyes using immobilized composite photocatalyst (2 wt.% of AC) (H_2O_2: 7.68 mM, BR18: dye: 0.128 mM, λ_{max}: 488 nm, pH: 5.5 and BR46: dye: 0.120 mM, λ_{max}: 532 nm, pH: 5.6).

Anion	BR18		BR46	
	k (min^{-1})	R^2	k (min^{-1})	R^2
No anion	0.0850	0.9878	0.1722	0.9764
Nitrate	0.0763	0.9977	0.1304	0.9861
Chloride	0.0746	0.9976	0.1315	0.9721
Sulfate	0.0770	0.9975	0.1281	0.9590
Bicarbonate	0.0492	0.9915	0.0990	0.9647
Carbonate	0.0241	0.9991	0.0423	0.9952

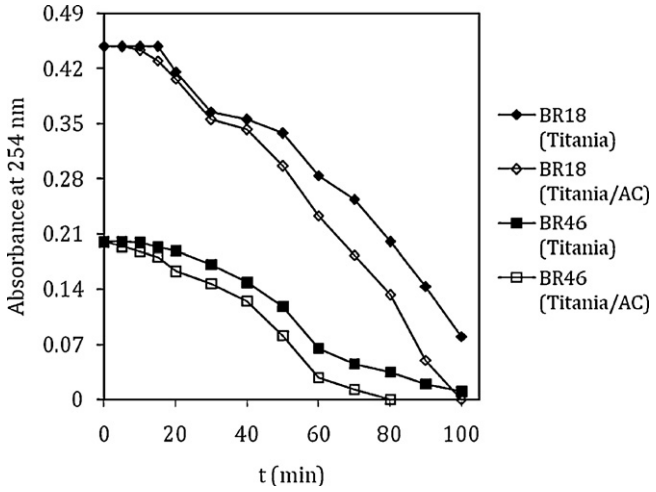

Fig. 11. Absorbance of the samples at 254 nm as an indication of the aromatic compound content during the photocatalytic degradation using immobilized titania and composite (titania/AC) photocatalysts (H_2O_2: 7.68 mM, BR18: dye: 0.128 mM, λ_{max}: 488 nm, pH: 5.5 and BR46: dye: 0.120 mM, λ_{max}: 532 nm, pH: 5.6).

should be evaluated as an overall degradation process, involving the degradation of both the parent dye and its intermediates.

Further hydroxylation of aromatic intermediates leads to the cleavage of the aromatic ring resulting in the formation of oxygen-

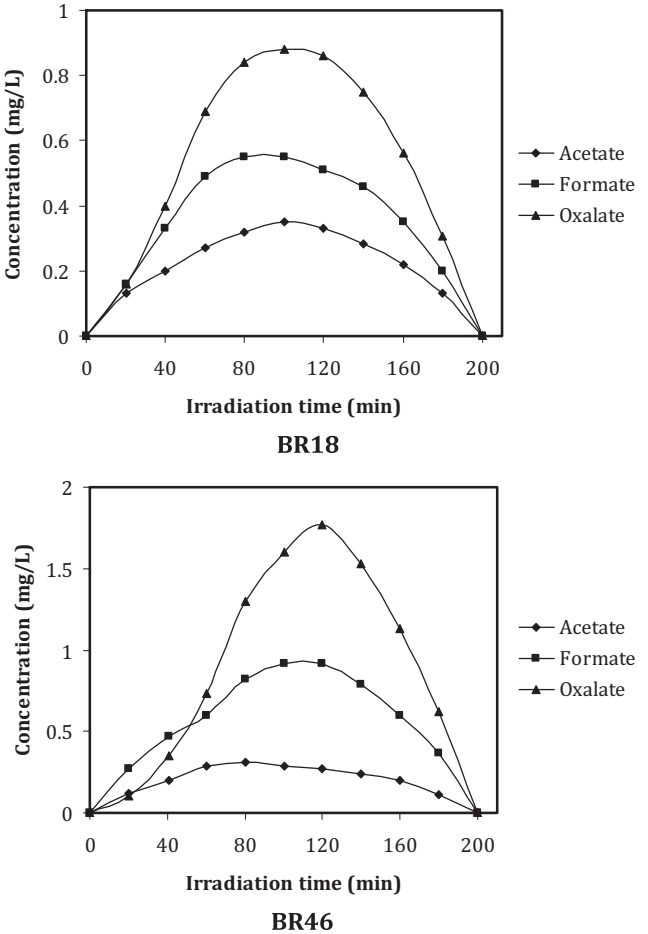

Fig. 12. Formation and disappearance of aliphatic carboxylic acids during the photocatalytic degradation of dyes using immobilized composite photocatalyst (2 wt.% of AC) (H_2O_2: 7.68 mM, BR18: dye: 0.128 mM, λ_{max}: 488 nm, pH: 5.5 andBR46: dye: 0.120 mM, λ_{max}: 532 nm, pH: 5.6).

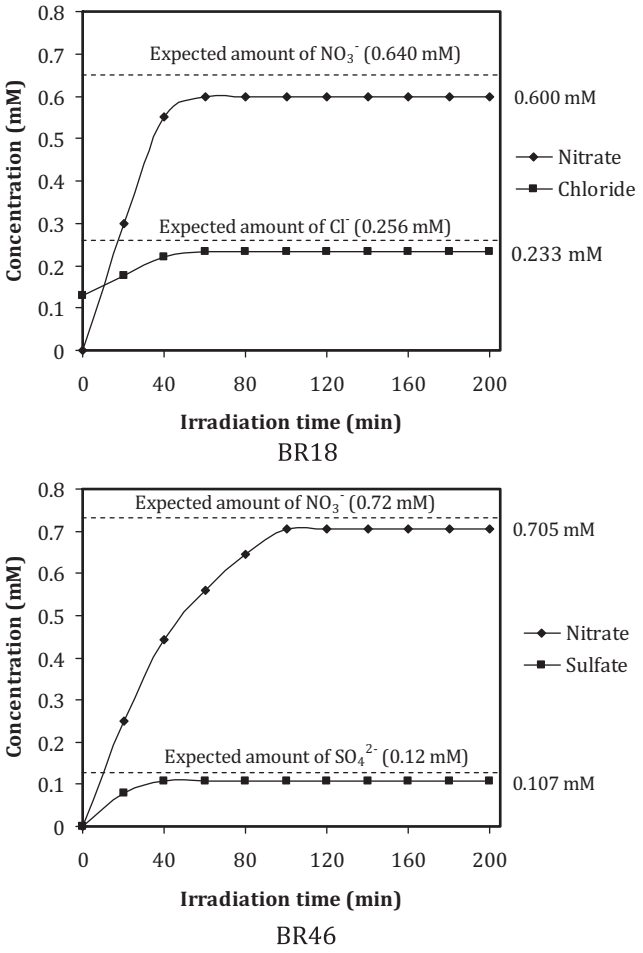

Fig. 13. Evolution of inorganic ions during the photocatalytic degradation of dyes using immobilized composite photocatalyst (2 wt.% of AC) (H_2O_2: 7.68 mM, BR18: dye: 0.128 mM, λ_{max}: 488 nm, pH: 5.5 and BR46: dye: 0.120 mM, λ_{max}: 532 nm, pH: 5.6).

containing aliphatic compounds [62]. Formate, acetate and oxalate were detected as important aliphatic carboxylic acid intermediates during the degradation of dyes (Fig. 12). The formation of oxalate initially increased with the illumination time, and then sharply dropped. Carboxylic acids can react directly with holes generating CO_2 according to the "photo-Kolbe" reaction:

$$R\text{–}COO^- + TiO_2(h_{VB}^+) \rightarrow TiO_2 + R^\bullet + CO_2 \quad (6)$$

Also, the photocatalytic mineralization of dye implies the appearance of inorganic products, mainly anions, since heteroatoms are generally converted into anions in which they are at their highest oxidation degree.

The dye degradation leads to the conversion of organic carbon into harmless gaseous CO_2 and that of N and S heteroatoms into inorganic ions, such as nitrate and sulfate ions, respectively [63]. Mineralization of dyes is reported for an irradiation period of 200 min. The formation of NO_3^-, SO_4^{2-} and Cl^- from dye mineralization was shown in Fig. 13.

The quantity of released nitrate ions (BR18: 0.600 mM and BR46: 0.705 mM) during the mineralization of dyes is lower than that expected from stoichiometry (BR18: 0.640 mM and BR46: 0.720 mM) indicating that N-containing species remain adsorbed in the photocatalyst surface or most probably, that significant quantities of N_2 and/or NH_3 have been produced and transferred to the gas-phase. In the azo bonds each nitrogen atom is in its +1 oxidation degree. This oxidation degree favors the evolution of gaseous N_2 by the two step reduction process expressed previously. N_2 evolution constitutes the ideal case for a decontamination reaction involving totally innocuous nitrogen-containing final product [10].

The quantity of released chloride ions (0.233 mM) during the mineralization of BR 18 is lower than that expected from stoichiometry (0.256 mM) indicating that chloride ions remain adsorbed onto the photocatalyst surface.

Finally, the quantity of released sulfate ions (0.107 mM) during the mineralization of BR46 is lower than that expected from stoichiometry (0.120 mM). This could be first explained by a loss of sulfur-containing volatile compounds such as H_2S and/or SO_2. However, this is not probable since both gases are very soluble in water and known as readily oxidizable into sulfate by photocatalysis. The more probable explanation for the quantity of SO_4^{2-} obtained smaller than that expected from stoichiometry is given by the partially irreversible adsorption of some SO_4^{2-} ions at the surface of titania as already observed. However, this partial adsorption of SO_4^{2-} ions does not inhibit the photocatalytic degradation of pollutants [10,63].

4. Conclusions

A novel immobilized composite photocatalyst, titania nanoparticle–*Canola* hull activated carbon (AC), was prepared and its photocatalytic activity on the degradation of textile dye in aqueous solution was tested. The reaction parameters studies showed that dyes were decolorized and degraded using novel immobilized composite photocatalyst. Aliphatic carboxylic acids were detected as dominant aliphatic intermediates where, they were further oxidized slowly to CO_2. Inorganic anions were detected as the photocatalytic mineralization products of dyes. Results show that novel immobilized composite photocatalyst is effective to degrade of textile dye. Thin-film coating of photocatalyst may resolve the problem of suspension system of decolorization. Hence, this technique may be a viable one for treatment of large volume of aqueous colored dye solutions. Photocatalysis using immobilized composite photocatalyst is able to decolorize and treat the colored textile wastewater without using high pressure of oxygen or heating.

References

[1] N.M. Mahmoodi, M. Arami, Chem. Eng. J. 146 (2009) 189–193.
[2] N.M. Mahmoodi, M. Arami, J. Photochem. Photobiol. B: Biol. 94 (2009) 20–24.
[3] H. Parab, M. Sudersanan, N. Shenoy, T. Pathare, B. Vaze, Clean 37 (2009) 963–969.
[4] N.M. Mahmoodi, M. Arami, J. Photochem. Photobiol. A: Chem. 182 (2006) 60–66.
[5] Y. Bulut, H. Aydın, Desalination 194 (2006) 259–267.
[6] N. Atar, A. Olgun, F. Çolak, Eng. Life Sci. 8 (2008) 499–506.
[7] N.K. Amin, J. Hazard. Mater. 165 (2009) 52–62.
[8] S. Rodríguez-Couto, J.F. Osma, J.L. Toca-Herrera, Eng. Life Sci. 9 (2009) 116–123.
[9] H. Zhu, R. Jiang, L. Xiao, Y. Chang, Y. Guan, X. Li, G. Zeng, J. Hazard. Mater. 169 (2009) 933–940.
[10] I.K. Konstantinou, T.A. Albanis, Appl. Catal. B: Environ. 49 (2004) 1–14.
[11] D.S. Bhatkhande, V.G. Pangarkar, A.A.C.M. Beenackers, J. Chem. Technol. Biotechnol. 77 (2001) 102–116.
[12] M.R. Hoffmann, S.T. Martin, W. Choi, D.W. Bahneman, Chem. Rev. 95 (1995) 69–96.
[13] S. Karuppuchamy, J.M. Jeong, J. Oleo Sci. 55 (2006) 263–266.
[14] F. Li, Y. Jiang, L. Yu, Z. Yang, T. Hou, S. Sun, Appl. Surf. Sci. 252 (2005) 1410.
[15] S. Fang, Y. Jiang, A. Wang, Z. Yang, F. Li, Chin. Non-Met. Mines 27 (1) (2004) 14.
[16] S. Fang, Y. Jiang, Y. Wang, C. Bao, B. Song, Chin. J. Environ. Sci. 24 (2003) 113.
[17] G.L. Puma, A. Bono, D. Krishnaiah, J.G. Collin, J. Hazard. Mater. 157 (2008) 209–219.
[18] K.E. O'Shea, E. Pernas, J. Saiers, Langmuir 15 (6) (1999) 2071–2076.
[19] R. Matthews, Sol. Energy 38 (1987) 405–413.
[20] N. Serpone, E. Borgarello, R. Harris, P. Cahill, M. Borgarello, Sol. Energy Mater. 14 (1986) 121–127.
[21] J. Sabate, M.A. Anderson, H. Kikkawa, M. Edwards, C.G. Hill, J. Catal. 127 (1991) 167–177.
[22] I.R. Bellobono, M. Bonardi, L. Castellano, E. Selli, L. Righetto, J. Photochem. Photobiol. A 67 (1992) 109–115.

[23] S. Tunesi, M. Anderson, J. Phys. Chem. 95 (1991) 3399–3405.
[24] R. Mariscal, J.M. Palacios, M. Galan-Ferreres, J.L.G. Fierro, Appl. Catal. A 116 (1994) 205–219.
[25] Y. Xu, H. Langford, J. Phys. Chem. 99 (1995) 11501–11507.
[26] Y.M. Gao, H.S. Shen, K. Dwight, A. Wold, Mater. Res. Bull. 27 (1992) 1023–1030.
[27] X. Zhang, M. Zhou, L. Lei, Carbon 44 (2) (2006) 325–333.
[28] M.L. Chen, C.S. Lim, W.C. Oh, J. Ceram. Process. Res. 8 (2007) 119–124.
[29] T. Cordero, J.-M. Chovelon, C. Duchamp, C. Ferronato, J. Matos, Appl. Catal. B: Environ. 73 (2007) 209–362.
[30] Y. Liu, S. Yang, J. Hong, C. Sun, J. Hazard. Mater. 142 (2007) 208–215.
[31] A.H. El-Sheikh, J.A. Sweileh, Talanta 71 (2007) 1867–1872.
[32] W. Wang, C.G. Silva, J.L. Faria, Appl. Catal. B: Environ. 70 (2007) 470–478.
[33] J. Matos, J. Laine, J.M. Herrmann, D. Uzcategui, J.L. Brito, Appl. Catal. B: Environ. 70 (2007) 461–469.
[34] C. Gomes da Silva, J.L. Faria, J. Photochem. Photobiol. A: Chem. 155 (2003) 133–143.
[35] M. Kubo, H. Fukuda, X.J. Chua, T. Yonemoto, Ind. Eng. Chem. Res. 46 (2007) 699–704.
[36] J. Araña, J.M. Doña-Rodrĭguez, E. Tello Rendón, C. Garriga i Cabo, O. González-Dĭaz, J.A. Herrera-Melián, J. Pérez-Peña, G. Colón, J.A. Navio, Appl. Catal. B: Environ. 44 (2003) 153–160.
[37] A.H. El-Sheikh, Y.S. Al-Degs, A.P. Newman, D.E. Lynch, Sep. Purif. Technol. 54 (2007) 117–123.
[38] X. Wang, Y. Liu, Z. Hu, Y. Chen, W. Liu, G. Zhao, J. Hazard. Mater. 169 (2009) 1061–1067.
[39] J. Matos, J. Laine, J.M. Herrmann, J. Catal. 200 (2001) 10–20.
[40] J. Matos, J. Laine, J.M. Herrmann, Appl. Catal. B: Environ. 18 (1998) 281–291.
[41] S.J. Park, S.S. Chin, Y. Jia, A.G. Fane, Desalination 250 (2010) 908–914.
[42] Y. Li, X. Li, J. Li, J. Yin, Catal. Commun. 6 (2005) 650–655.
[43] Y. Gao, H. Liu, Mater. Chem. Phys. 92 (2005) 604–608.
[44] A.K. Ray, A.A.C.M. Beenackers, AIChE J. 44 (2) (1998) 477–483.
[45] APHA, Standard Methods for the Examination of Water and Wastewater, 17th ed., American Public Health Association, Washington, DC, 1989.
[46] D.L. Pavia, G.M. Lampman, G.S. Kaiz, Introduction to Spectroscopy: A Guide for Students of Organic Chemistry, W.B. Saunders Company, 1987.
[47] D. Mohan, K.P. Singh, S. Sinha, D. Gosh, Carbon 43 (2005) 1680–1693.
[48] J. de Celis, N.E. Amadeo, A.L. Cukierman, J. Hazard. Mater. 161 (2009) 217–223.
[49] A.A. Nunes, A.S. Franca, L.S. Oliveira, Bioresour. Technol. 100 (2009) 1786–1792.
[50] J.M. O'Reilly, R.A. Mosher, Carbon 21 (1983) 47–51.
[51] K. Vinodgopal, I. Bedja, S. Hotechandani, P.V. Kamat, Langmuir 10 (1994) 1767–1771.
[52] C.M. So, M.Y. Cheng, J.C. Yu, P.K. Wong, Chemosphere 46 (2002) 905–912.
[53] S. Malato, J. Blanco, C. Richter, B. Braun, M.I. Maldonado, Appl. Catal. B: Environ. 17 (1998) 347–356.
[54] J. Li, C. Chen, J. Zhao, H. Zhu, J. Orthman, Appl. Catal. B: Environ. 37 (2002) 31–338.
[55] C.G. da Silva, J.L. Faria, J. Photochem. Photobiol. A: Chem. 155 (2003) 133–143.
[56] F. Zhang, J. Zhaoa, T. Shen, H. Hidaka, E. Pelizzetti, N. Serpone, Appl. Catal. B: Environ. 15 (1998) 147–156.
[57] B. Neppolian, H.C. Choi, S. Sakthivel, B. Arabindoo, V. Murugesan, J. Hazard. Mater. B89 (2002) 303–317.
[58] W.Z. Tang, Z. Zhang, H. An, M.O. Quintana, D.F. Torres, Environ. Technol. 18 (1997) 1–12.
[59] C. Tang, V. Chen, Water Res. 38 (2004) 2775–2781.
[60] I. Arsalan-Alaton, Color Technol. 119 (2003) 345–353.
[61] D. Georgiou, P. Melidis, A. Aivasidis, K. Gimouhopoulos, Dyes Pigments 52 (2002) 69–78.
[62] K. Tanaka, S.M. Robledo, T. Hisanaga, R. Ali, Z. Ramli, W.A. Bakar, J. Mol. Catal. A: Chem. 144 (1999) 425–430.
[63] A. Houas, H. Lachheb, M. Ksibi, E. Elaloui, C. Guillard, J.M. Hermann, Appl. Catal. B: Environ. 31 (2001) 145–157.